ELSEVIER

Materials Science and Engineering B 137 (2007) 184–188

MATERIALS SCIENCE & ENGINEERING B

www.elsevier.com/locate/mseb

Preparation, structure and dielectric property of barium stannate titanate ceramics

Xiaoyong Wei *, Xi Yao

Electronic Materials Research Laboratory, Key Laboratory of the Ministry of Education, Xi'an Jiaotong Univesity, Xi'an 710049, People's Republic of China

Received 28 May 2006; received in revised form 1 November 2006; accepted 6 November 2006

Abstract

The processing route of barium stannate titanate ceramics were optimized to prepare full composition range solid solution sample. The phase structure, microscopic morphology and dielectric properties of barium stannate titanate ceramics were studied. X-ray diffraction patterns indicated that the samples are of single perovskite structure. Linear empirical relationship between crystal lattice and tin content was proposed. This relationship is valid covering the full composition range, which suggests that this solid solution system is ultimate mutual soluble. The phase transition behavior was studied and a phase diagram was obtained based on the dielectric measurements.

Keyword: Barium stannate titanate

1. Introduction

Barium stannate titanate (BTS) ceramics was studied by Smolensky [1] at the early 1970s as a prototype of ferroelectrics with diffused phase transition. In the next 20 years, few papers were published involving BTS. Since 1990, although several works had been reported on ceramics [2–5] and thin film [6–10] preparation, and on phase transition [3,4,11–14], electromechanical [15–17], electrical [18,19] and dielectric [3,20–24] properties, the common academic attention is fairly insufficient compared with that of barium strontium titanate.

BTS is a binary solid solution system composed of ferroelectric barium titanate and non-ferroelectric barium stannate. Both of them are of perovskite structures with an ABO_3 formula. The B sites of the solid solution are occupied by either titanium or tin ions. This material system may find application for various purposes because the Curie temperature or dielectric maximum can be widely shifted by changing the tin content. The permittivity is very high and as well temperature as bias field sensitive. Therefore, it can be used in various potential applications, such as capacitor, bolometer, actuator [16,17] and microwave phase shifter [22–24].

Yasuda et al. [3] had extensively studied the phase transition behavior, dielectric and ferroelectric properties of BTS. However, in his study, the highest solubility of barium stannate is only 0.4. Therefore, a systematically study covering the whole range is required. The sintering temperature of BTS ceramics is as high as 1500 °C and the grain growth is extremely inhomogeneous [23]. Thus, the processing route in solid state reaction needs to be optimized.

In the present paper, the processing route was optimized to prepare full range solid solution sample $Ba(Sn_xTi_{1-x})O_3$ ($x = 0$–1), and the phase structure, microscopic morphology and dielectric properties of BTS ceramics were studied.

2. Experiment

The BTS ceramic sample was prepared by means of solid state synthesis. The raw materials are reagent grade $BaCO_3$ (99.9%, Fenghua), TiO_2 (99.8%, Fenghua), SnO_2 (99.8%, Northwest Institute of Non-Ferric Metal) and hydrothermal synthesized spherical particle $BaTiO_3$ (Guoteng). The notations and formulas of the selected compositions of BTS solid solution are shown in Table 1.

The raw materials were weighed and ball milled, then calcined at 1000–1100 °C for 3 h. The synthesized powder was ball milled again before pressed into pellets, and densified to ceramics by sintering at 1250–1500 °C for 2 h.

* Corresponding author. Tel.: +86 29 82668679; fax: +86 29 82668794.
E-mail address: wdy@mail.xjtu.edu.cn (X. Wei).

0921-5107/$ – see front matter © 2006 Elsevier B.V. All rights reserved.
doi:10.1016/j.mseb.2006.11.012

Table 1
Compositions of BTS solid solution

Notation	Formula	Sintering parameters	Density		Resistivity (Ω cm)
			Absolute (g/cm^3)	Relative (%)	
BTS0	$BaTiO_3$	1250 °C/2 h	5.81	96	10^{10}
BTS6	$Ba(Ti_{0.94}Sn_{0.06})O_3$	1300 °C/2 h	5.91	97	10^{11}
BTS10	$Ba(Ti_{0.90}Sn_{0.10})O_3$	1380 °C/2 h	6.04	98	10^{12}
BTS20	$Ba(Ti_{0.80}Sn_{0.20})O_3$	1380 °C/2 h	6.14	97	10^{12}
BTS30	$Ba(Ti_{0.70}Sn_{0.30})O_3$	1420 °C/2 h	6.24	97	10^{12}
BTS40	$Ba(Ti_{0.60}Sn_{0.40})O_3$	1420 °C/2 h	6.29	96	10^{12}
BTS50	$Ba(Ti_{0.50}Sn_{0.50})O_3$	1420 °C/2 h	6.34	95	10^{11}
BTS60	$Ba(Ti_{0.40}Sn_{0.60})O_3$	1450 °C/2 h	6.43	95	10^{11}
BTS70	$Ba(Ti_{0.30}Sn_{0.70})O_3$	1450 °C/2 h	6.57	95	10^{13}
BTS80	$Ba(Ti_{0.20}Sn_{0.80})O_3$	–	6.63	94	10^{12}
BTS90	$Ba(Ti_{0.10}Sn_{0.90})O_3$	–	6.60	92	10^{11}
BTS100	$BaSnO_3$	–	–	–	10^{10}

The phase structure of the ceramic sample was determined using a powder X-ray diffractometer (XRD/Dmax2400, Rigaku). The microscopic morphology was analyzed by a scanning electronic microscope (SEM/1000B, Amray). The density of the sample was measured using Archimedean method with an electronic balance (Mettler-Toledo). The temperature dependence of dielectric constant was measured using a LCR meter (HP4284A, Hewllet-Packard) and a temperature chamber. The direct current resistivity was measured by an ohmic meter (HP4339, Hewllet-Packard).

3. Results

3.1. Starting material selection and sintering temperature optimization

There were three processing routes to synthesize BTS powder: (a) started from raw materials $BaCO_3$, TiO_2 and SnO_2; (b) started from hydrothermal $BaTiO_3$, raw materials $BaCO_3$ and SnO_2; (c) started from hydrothermal $BaTiO_3$ and pre-synthesize $BaSnO_3$, which was pre-calcined from $BaCO_3$ and SnO_2 at 1200 °C for 4 h showing single perovskite structure and 602 nm average particle size.

The phase structures of the three types of calcined powders were analyzed by XRD. The resultants of routes A and B were single phase perovskite, while a small amount of residual barium stannate was detected in the resultant of route C indicating an incomplete synthesis, although all the final sintered ceramics were of single phase perovskite structure. The microscopic morphology of ceramics prepared via route A showed inhomogeneous and abnormal grain growth, while that of routes B and C were homogeneous. Therefore, route B was selected as the optimized one.

Sintered ceramic bodies, covering the whole solution range, were prepared following the route B starting from hydrothermal $BaTiO_3$, raw materials $BaCO_3$ and SnO_2. The absolute and relative densities are listed in Table 1. When the tin content is higher than 80%, it is noticed that the ceramics are not fully densified, which is proved by apparent observation and noticeable dielectric loss at room temperature, in spite of the measured high relative density.

BTS6 ($Ba(Sn_{0.06}Ti_{0.94})O_3$) ceramics was selected for sintering temperature optimization ranged from 1250 to 1425 °C with a step of every 25 °C. The results are listed in Table 2. The maximum density was obtained at 1300 °C; the grain size increased with increasing temperature which is calculated from the cutting lines in the SEM photos; the room temperature dielectric constant decreased with the increasing temperature which is something related to the inner-granular stress; the resistivity was measured using a HP4339 high resistance meter and the highest resistivity was obtained in sample sintered at 1300 °C. These results suggest that the optimized sintering temperature is in the vicinity of 1300 °C.

The SEM morphology of the fracture faces of BTS10 ($Ba(Sn_{0.10}Ti_{0.90})O_3$) and BTS20 ($Ba(Sn_{0.20}Ti_{0.80})O_3$) are shown in Fig. 1. It can be seen that well grown and homogeneous grain structure and dense ceramic body can be obtained via processing route B.

3.2. Phase determination and lattice constant refinement

As shown in Fig. 2, the XRD patterns indicate that all the samples are of single phase perovskite structure. Except for barium titanate, the non-cubic peak splitting can not be detected for the other compositions (tin content ≥ 10%) even in those high angle refraction peaks. This is in agreement with that reported

Table 2
Influence of sintering temperature of BTS6

Sintering temperature (°C) (duration 2 h)	1250	1275	1300	1325	1350	1375	1400	1425
Density (g/cm^3)	5.67	5.81	5.91	5.89	5.87	5.85	5.87	5.87
Grain size (um)	3	6	10	15	16	14	19	18
Dielectric constant	3226	3074	2809	2761	2484	2669	2514	2566
Resistivity (10^{10} Ω cm)	5	30	30	20	10	2	1	1

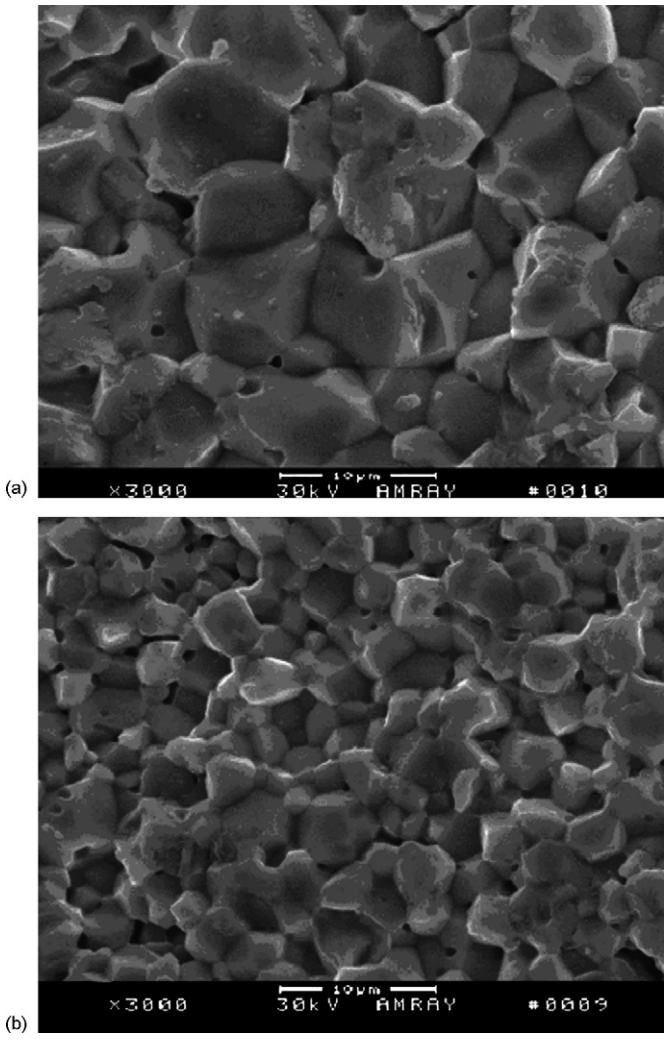

Fig. 1. SEM morphology of fractured faces of: (a) BTS10 and (b) BTS20.

by Yasuda et al. [3]. The results of refinement of crystal lattice constant are shown in Fig. 3. The extrapolation function is $(\cos^2\theta)/((1/\sin\theta)+(1/\theta))$, and the peak data used are in range of high refraction angle ($2\theta = 60$–110°). The fitting results exhibit well fitted linear relationship between lattice constant and tin content. The fitting equation of lattice constant is

$$a = 4.0046 + 0.0011x \ (\text{Å}) \quad (1)$$

where a represents lattice constant or the cubic root of crystal cell volume (for tetragonal symmetry only) and x is the percentage of tin content.

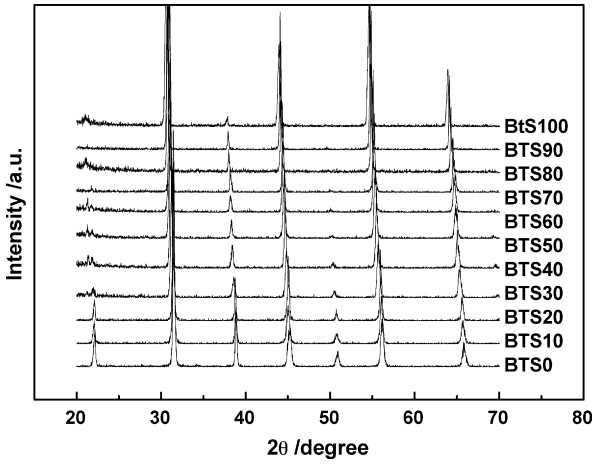

Fig. 2. XRD patterns of BTS solid solution.

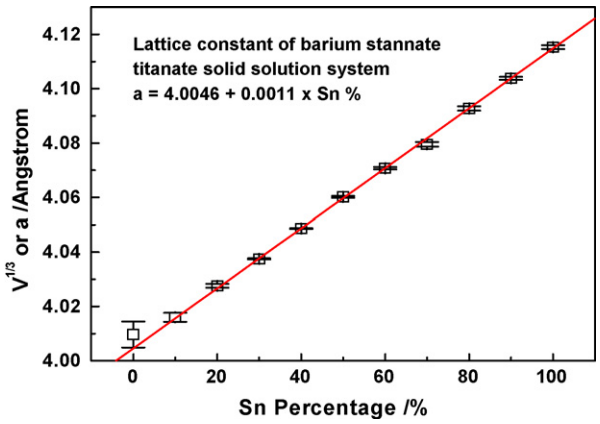

Fig. 3. Lattice constant of BTS as a function of the tin content.

3.3. Dielectric properties and phase diagram

The temperature dependences of dielectric constant of BTS ceramic samples are shown in Fig. 4. The dielectric maxima decrease with increasing tin content, with a rate of roughly 8 °C per centesimal B site substitution. When the tin content exceeds 40%, the phase transition temperature is lower than the temperature of liquid nitrogen, the low temperature limit in our experiment. The dielectric peaks of phase transition becomes diffused when the tin content is larger than 10%, and relaxation behavior can be observed in the sample with the tin content equal to 30%.

This solid solution system is a combination of ferroelectric and non-ferroelectric perovskite structures. The common schematic phase diagram of this type of solid solution had been predicted by Cheng [25]. We plotted a phase diagram of BTS based on the dielectric measurements, as shown in Fig. 5, which is similar to both that proposed by Yasuda et al. [3] and predicted by Cheng. As we know in case of barium titanate, there are several dielectric peaks, which illustrate successive phase transitions from cubic, tetragonal and orthorhombic to rhombohedral crystal lattice. When the tin content is larger than 10%, there is only one dielectric peak, which indicates there is only one rhombohedral ferroelectric phase. When the tin content is more than 25%, there are dielectric relaxation in phase transition region [22], thus the phase transition temperature is expanded to a temperature region.

3.4. P–E hysteresis loop

The polarization hysteresis loops of BTS20 were measured at various temperatures as shown in Fig. 6. In ferroelectric

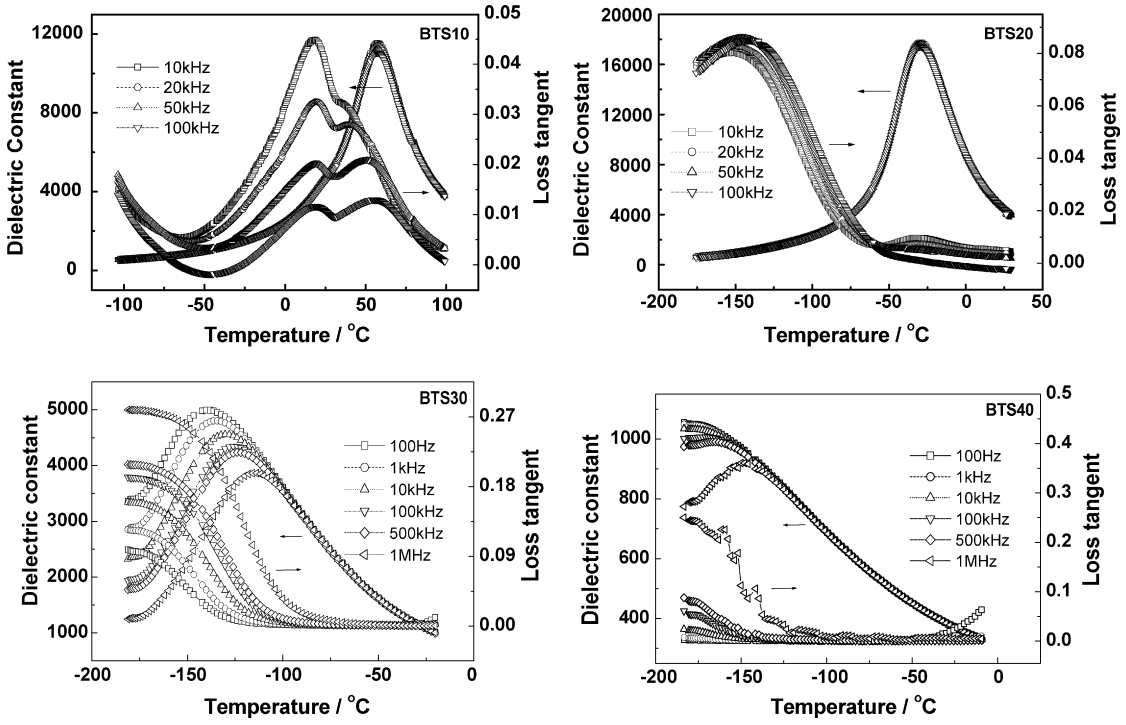

Fig. 4. Temperature dependence of dielectric constant of BTS samples.

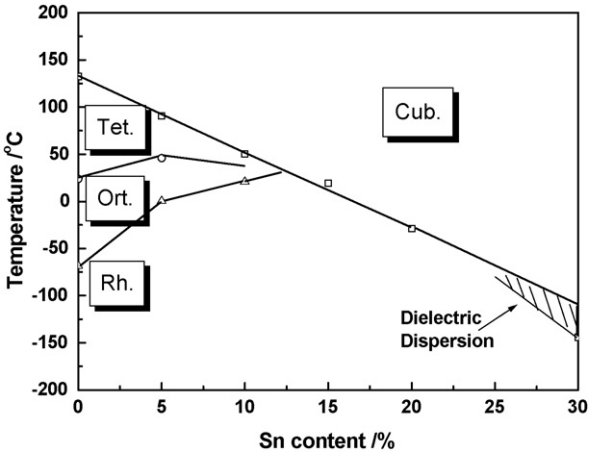

Fig. 5. Phase diagram of BTS based on dielectric measurments.

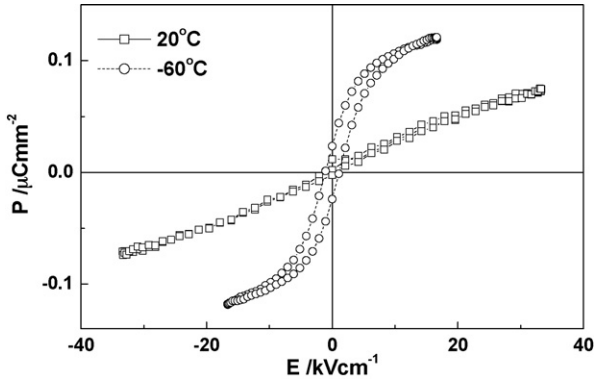

Fig. 6. *P–E* hystersis loops of BTS20 ceramics.

phase (−60 °C) of BTS20, the hysteresis loop indicates normal ferroelectricity with weak remanent polarization. While in its paraelectric phase (20 °C), the loop looks like S shape line.

4. Discussions

The linearship between lattice constant and tin content (Eq. (1)) indicates a good structural compatibility between barium titanate and barium stannate, and the crystal lattice constant of BTS solid solution obeys Vegard Law, which features a linear relationship covering full solution range. Therefore, these results suggest that this solid solution system is ultimate mutual soluble.

As shown in Fig. 4, it is obvious that the dielectric relaxation behavior of the sample is closely related to the tin content. The degrees of relaxation and diffuseness had been quantitatively analyzed elsewhere [22/CI1397]. On introducing FDDP, a parameter for dielectric dispersion, the relaxor behavior is supposed to be observable if the FDDP inflexion temperature is close to the phase transition region in BTS samples. This can be understood in view of that the relaxation behavior is originated from polar nanoregions. Dielectric relaxation behavior can be observed only if the measurement frequency is close to the relaxation frequency of the polar nanoregions. Otherwise, there is no relaxation behavior even if the dielectric peak is diffused [22].

With addition of tin atoms in B site of perovskite cells, the ferroelectricity of BTS is diluted. Thus, as shown in Fig. 6, for one-fifth tin occupancy in B site (BTS20), the remanent spontaneous polarization in the ferroelectric region was weakened drastically compared to that of barium titanate. While for BTS10, in its ferroelectric phase, there is a temperature region

where the loops are slim-waist shaped. We are convinced it is related with interaction between defects and domain walls. When field is decreased after domains were fully orientated, point defects may drive domain walls back to the original positions and thus produce the abnormal *P–E* loops [22].

5. Conclusion

Dense and well sintered BTS ceramics were prepared using optimized solid reaction route. XRD patterns indicated that the samples are of single perovskite structure. Linear empirical relationship between crystal lattice and tin content was proposed. This relationship is valid covering the full composition range, which suggests that this solid solution system is ultimate mutual soluble.

References

[1] G.A. Smolensky, J. Phys. Soc. Jpn. 28 (Suppl.) (1970) 26.
[2] M.L. Bao, W.D. Li, P.N. Zhu, J. Mater. Sci. 28 (1993) 6617.
[3] N. Yasuda, H. Ohwa, S.H. Asano, Jpn. J. Appl. Phys. 35 (1996) 5099.
[4] W.K. Chang, S.F. Hsieh, Y.H. Lee, K.N. Chen, N.C. Wu, A.A. Wang, J. Mater. Sci. 33 (1998) 1765.
[5] W. Chen, B. Liu, Q.F. Liu, S.T. Chen, J. Chin. Ceram. Soc. 28 (2000) 1999.
[6] M. Tsukada, M. Mukaida, S. Miyazawa, Jpn. J. Appl. Phys. 35 (1996) 4908.
[7] K.H. Yoon, J.H. Park, J.H. Jang, J. Mater. Res. 14 (1999) 2933.
[8] S. Halder, P. Victor, A. Laha, S. Bhattacharya, S.B. Krupanidhi, G. Agarwal, A.K. Singh, Solid State Commun. 121 (2002) 329.
[9] H.H. Huang, M.C. Wang, C.Y. Chen, N.C. Wu, H.J. Lin, J. Eur. Ceram. Soc. 26 (2006) 3211.
[10] H.J. Lin, H.H. Huang, C.Y. Chen, N.C. Wu, M.C. Wang, Jpn. J. Appl. Phys. 45 (Pt1) (2006) 7002.
[11] K. Toyoda, T. Kato, Y. Sakabe, Ferroelectrics 108 (1990) 227.
[12] K.Y. Oh, K. Uchino, L.E. Cross, J. Am. Ceram. Soc. 77 (1994) 2809.
[13] N. Baskaran, H. Chang, J. Mater. Sci. 12 (2001) 527.
[14] V. Mueller, L. Jager, H. Beige, H.P. Abicht, T. Muller, Solid State Commun. 129 (2004) 757.
[15] J.V. Cieminski, H.T. Langhammer, H.P. Abicht, Phys. Status Solidi (a) 120 (1990) 285.
[16] U. Straube, H.T. Langhammer, H.P. Abicht, H. Beige, J. Eur. Ceram. Soc. 19 (1999) 1171.
[17] R. Steinhausen, A. Kouvatov, H. Beige, H.T. Langhammer, H.P. Abicht, J. Eur. Ceram. Soc. 24 (2004) 1677.
[18] R. Vivekanandan, T.R.N. Kutty, Mater. Sci. Eng. B 6 (1990) 221.
[19] C. Kajtoch, Mater. Sci. Eng. B 64 (1999) 25.
[20] N. Yasuda, H. Ohwa, K. Arai, M. Iwata, Y. Ishibashi, J. Mater. Sci. Lett. 16 (1997) 1315.
[21] V. Mueller, H. Beige, H.P. Abicht, Appl. Phys. Lett. 84 (2004) 1341.
[22] X.Y. Wei, Y.J. Feng, X. Yao, Appl. Phys. Lett. 83 (2003) 2031;
X.Y. Wei, Y.J. Feng, X. Yao, Appl. Phys. Lett. 84 (2004) 1534;
X.Y. Wei, Y.J. Feng, X. Wan, X. Yao, Ceram. Int. 30 (2004) 1397;
X.Y. Wei, Y.J. Feng, L.M. Hang, X. Yao, Ceram. Int. 30 (2004) 1401;
X.Y. Wei, X. Yao, J. Electroceram., in press;
X.Y. Wei, L. Jin, X. Yao, Appl. Phys. Lett. 87 (2005) 082905;
X.Y. Wei, Y.J. Feng, L.M. Hang, S. Xia, L. Jin, X. Yao, Mater. Sci. Eng. B 120 (2005) 64.
[23] X.Y. Wei, Ph.D. Thesis, Xi'an Jiatong Unviersity, 2005.
[24] S.G. Lu, Z.K. XU, H. Chen, Appl. Phys. Lett. 85 (2004) 5319.
[25] Z.Y. Cheng, Ph.D. Thesis, Xi'an Jiaotong Univesity, 1994.